Nanostructured Magnets and High Power Density Synchronous Generators

Sergey E. Lyshevski

Department of Electrical and Microelectronic Engineering
Rochester Institute of Technology
Rochester, NY 14623 USA
E-mail: Sergey.Lyshevski@mail.rit.edu
URL: http://people.rit.edu/seleee www.rit.edu/kgcoe/staff/sergey-lyshevski

ABSTRACT

This paper examines nanostructured magnets for highperformance synchronous generators and electric machines. The unique magnetic phenomena, as well as mechanical and chemical properties, of the iron alloys and lanthanide rare earths elements are utilized in magnets. It is important to develop new paradigms and advance the existing technologies, including iron alloys and iron oxides (strontium and barium ferrites) magnets. There are needs to develop practical and alternative solutions departing from rare earths magnets. The premises of interacting hard and soft phases with magnetic exchange coupling and energy product enhancement are still under developments. We study recent advances in magnets with nanocrystalline and nanophase structures based on rare-earth and iron alloys. The nanocrystalline single-phase and nanocomposite $R_2Fe_{14}B$-based magnets (R=rare earth elements), NdFe, NdFeB, R_2Co_{17} and RCo_5 magnets, $Sm(Fe,M)_{12}$ (M=Ti,V,Mo), $Nd(Fe,M)_{12}$ and other magnets are evaluated. The energy product, remanence, coercivity, magnetization, magnetic hardening, morphologies (microstructure, composition, grain size, phase constitution, etc.) of nanostructured magnets affect electric machine and transducer performance. We design and examine synchronous machines. Our findings are justified and substantiated by experimental studies.

Keywords: energy, electric machine, magnets, nanoindentation, synchronous generator

1. INTRODUCTION

This paper examines enabling solutions for power generation systems to improve and empower *clean* and renewable energy systems. We study electric machines with advanced-technology and nanostructured magnets. Optimized-by-design Alnico alloy magnets meet the specifications for high-energy-density high-performance synchronous generators. Generators should guarantee safety, affordability, optimal energy conversion, minimal losses, maximum power density, overloading, minimal cogging torque, etc.

Magnets and electric machine analysis, design and compliance are subject of intensive research [1, 2]. One characterizes and selects magnets using the energy product $(BH)_{max}$, remanence B_r, magnetization, coercivity H_c, temperature stability, robustness, etc. While the N52 grade $Nd_2Fe_{14}B$ have the highest $(BH)_{max}$ and remanence B_r, the NdFeB magnets do not guarantee the best electric machine performance [1]. The exchange-coupled nanocomposite magnets are considered as a possible inroad. However, this premise was not tested and substantiated in electric machines. The inter-phase exchange effectiveness, $(BH)_{max}$ phase preservation, stability, manufacturability, assembly and other issues are open. Using the wet chemistry and ball milling, ~20 nm nanoparticle composites should be self-organized and assembled. Challenges arise in maintaining uniformity, crystal structure consistency, magnetic alignment, etc. We focus on consistent technologies and practical solutions.

2. NANOSTRUCTURED MAGNETS

Advanced electric machines require permanent magnets with adequate coercivity, magnetic flux, energy product, stability, etc. [1-3]. The Alnico magnets have sufficient remanent force B_r and coersivity H_c, excellent corrosion resistance, high Curie temperature, robustness, etc. [1, 4, 5]. Coercivity may be increased by controlling composition, matching particles to a single-domain size, etc. Currently, ~100 nm to μm powders are produced using ball milling, while, nanoparticles can be prepared by hydrogen plasma metal reaction and other processes. The particle size and microstructure correspondence to the optimal magnetic properties are determined. The Alnico 5-7 (B_r=1.35 T, H_c=58.9 kA/m) and Alnico 9 (B_r=1.12 T, H_c=109.4 kA/m) compositions in % are $Fe_{49.9}$,$Co_{24.3}$,Ni_{14},$Al_{8.2}$,$Cu_{2.3}$,Nd_1 and $Fe_{35.5}$,$Co_{35.4}$,$Ni_{13.1}$,Al_7,$Cu_{3.2}$,$Nd_{0.5}$,Ti_5 [6, 7].

In Alnico 5-7 and 9, most composite grains are aligned along the [0 0 1] direction. The commercial-grade Alnico alloys with nanostructured spinodal decomposed phases were characterized in [6, 7]. The spinodal phase assembly is sensitive to alloy chemistry and processing. The Alnico alloys structure, ordering, alignment and compositions are

different. Titanium changes the α_2 phase from B2-ordered structure in Alnico 5-7 to $L2_1$-ordered structure in Alnico 9 [6, 7]. Copper changes the α_1 and α_2 phases. The saturation magnetization and coercivity depend on α_1 and α_2 phases, interacting domains, dimensionality, etc. The Alnico nanostructured magnets can be designed-by-specifications. The electric machines are optimized by electromagnetic design and magnetic system optimization.

3. MAGNETS: MECHANICAL PROPERTIES

The magnetic characteristics and quantities of Alnico magnets are reported in [1-7]. We examine the mechanical properties, and, find the elastic modulus and hardness of Alnico alloys from load-displacement measurements. The surface hardness H is $H=P/A$, where P is the load applied to the test surface; A is the contact area.

Using nanoindentation test of the sample, the Young modulus E is found from the reduced modulus E_r which is given as [8, 9] $E_r = \frac{\sqrt{\pi}S}{2\beta\sqrt{A_h}}$, where β is the constant which depends on the indenter geometry; A_h is the projected area of the indentation at the contact depth h.

The elastic modulus E is calculated using the expression

$$\frac{1}{E_r} = \frac{1-\nu^2}{E} + \frac{1-\nu_i^2}{E_i},$$

where ν is the Poisson's ratio of the test material; E_i and ν_i are the elastic modulus and Poisson's ratio of the indenter. For diamond, E_i=1141 GPa and ν_i=0.07. For indenters with triangular cross sections tip-geometry (the Berkovich indenters), β=1.034.

The Alnico sample is mounted onto a sample stub and analyzed using instrumented indentation testing on an MTS Nanoindenter XP. High resolution is achieved due to the ability to position indents within 1 micron of each other. This tool functions by employing a high resolution actuator to force an indenter into the sample surface. Simultaneously, a high resolution sensor continuously measures the resulting penetration. Hardness and elastic modulus and creep (deformation) are measured.

The samples are conditioned at least 12 hours at 70°F, 50% relative humidity prior to testing. After conditioning, 5 indentations are generated using a range of load conditions from 25 to 400 mN. The device is equipped with a 5 micron radius 60 degree conical diamond Berkovich tip. The modulus, hardness, maximum displacement and standard deviation are determined for each sample using the TestWorks® software. The instrument is calibrated using the fused silica with E=74.6 GPa (the nominal elastic modulus of fused silica is 72 GPa).

We examine the mechanical properties of the Alnico alloys using nanoindentation and AFM analyses. A typical load–displacement curves showing continuous displacement as indenter is driven into material up to maximum load 400 mN are documented in Figure 1. At maximum loads, the load is held constant for 30 seconds after which unloading begins. The charts of Alnico alloy hardness and modulus as functions of the load are reported in Table 1 and Figures 2.

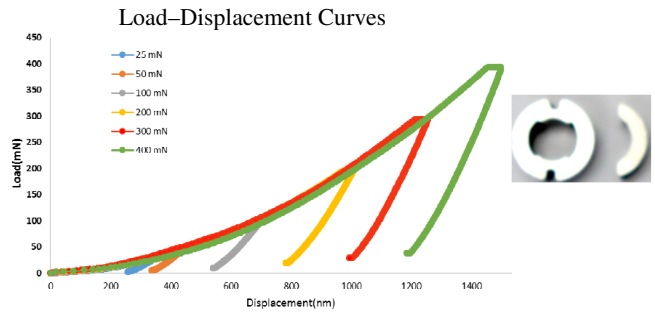

Figure 1. Load–displacement curves at six load conditions showing continuous displacement as indenter is driven into Alnico 5-7 alloy

Table 1. Displacement, Hardness and Modulus for Different Applied Loads

Load [mN]	Displacement [nm]		Hardness [GPa]		Modulus [GPa]	
	Average	Standard Deviation	Average	Standard Deviation	Average	Standard Deviation
25	332.101	25.823	10.394	1.607	250.249	41.436
50	461.337	35.811	11.694	2.021	263.498	20.708
100	700.221	27.638	10.309	0.616	245.402	21.541
200	1000.05	27.728	10.362	0.785	244.113	5.16
300	1239.79	85.902	10.123	1.48	257.438	32.866
400	1494.27	38.259	9.227	0.516	234.69	14.379
Average			10.35	1.17	249.23	22.68

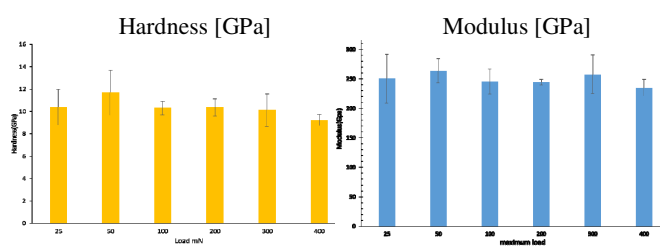

Figure 2. Charts of Alnico alloy hardness and modulus at different loads: The average hardness and modulus are 10.35 GPa and 249.23 GPa

The AFM images of the Alnico surfaces are reported in Figures 3 and 4.

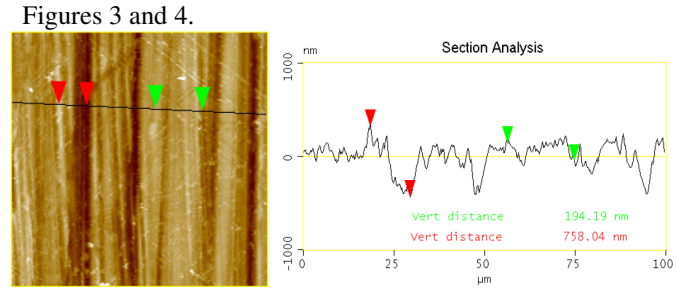

Figure 3. The Alnico surface roughness reaches ~180 nm. The rms surface roughness is ~88nm.

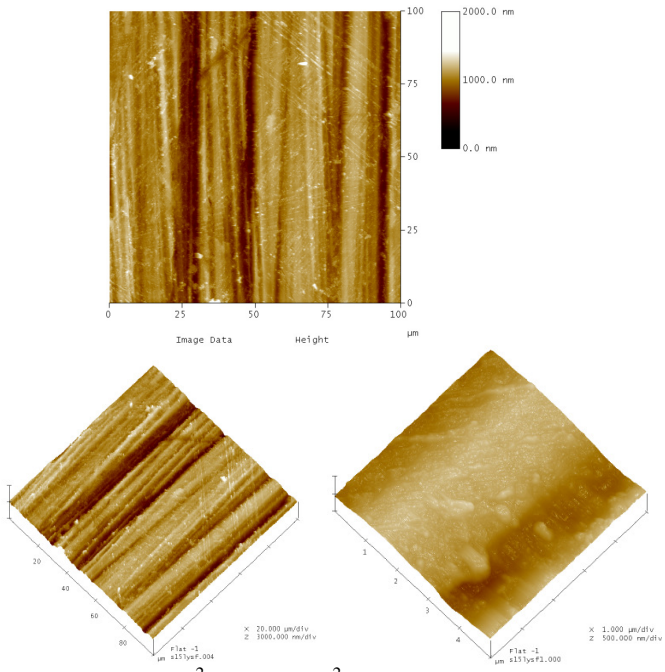

Figure 4. 100 μm^2 and 5 μm^2 AFM images: There are nanostructured composites, including long grains, on the Alnico surface.

4. SYNCHRONOUS GENERATORS

The studied nanostructured magnets [1-7] for permanent-magnet generators [1, 2]. These generators can be used in light-, medium- and heavy-duty commercial and industrial power generation systems from 1 to more than 100 kW rated. The proposed solutions also uniquely suit automotive, aerospace, naval and other systems. The studied high power density generators are used in wind, hydro, nuclear and other power generation systems.

High energy, high power and high torque densities electric machines and transducers require application-specific magnets with required characteristics. In high performance actuators and generators, the rare-earth SmCo and NdFeB magnets are commonly used due to high energy product $(BH)_{\max}$. However, these magnets may not ensure adequate thermal stability, must be coated to prevent corrosion, brittle, sensitive to mechanical impact, prone to chipping and cracking, etc. Moreover, rotors and stators are made from high permeability laminated electric steel. One increases the air gap with attempts to ensure uniform near-sinusoidal magnetic coupling, as well as to reduce varying reluctance, torque ripple, cogging and other undesired phenomena. The nanostructured Alnico magnets may meet the spectrum of requirements and ensure performance compared with, or, surpassing rare-earth magnets. One may refine magnetic domains, magnetic anisotropy, crystallographic alignment, crystalline structure and microstructure (composition, size, texture, separation, etc.) in order to control and optimize magnet characteristics.

The nanostructured Alnico magnets have sufficient energy product $(BH)_{\max}$, high remanent force (B_r), superior corrosion resistance, high Curie and operating temperatures, etc. High $(BH)_{\max}$ and coercive force H_c are achieved by decreasing particle size because the maximum values correspond to the single-domain size (acicular Co-Ni crystal diameter is ~30 to 50 nm with interparticle spacing ~50 nm). The micrometer size is achieved by using ball milling, while, nanoparticles are prepared by hydrogen plasma metal reaction. Alnico 5, 5-7 and 9 with the particle diameter from ~20 to 40 nm are examined. The nanoparticles have the same crystalline structure and lattice parameter as powdered metallurgical sintered (H_c and $BH_{\max}$ are ~50 kA/m and 35 kJ/m^3) and cast (H_c and $BH_{\max}$ are ~55 kA/m and ~50 kJ/m^3) Alnico alloys. The *JH* and *BH* curves are reported in [1]. Optimal design of Alnico magnets for synchronous machines is performed.

Using three-dimensional Maxwell's equations and tensor analysis, the synchronous machine electromagnetic system is optimized. The consistently-designed and optimized permanent-magnet synchronous motors and generators are examined using the Kirchhoff voltage laws [1, 2]

$$\mathbf{u}_{abcs} = \mathbf{r}_s \mathbf{i}_{abcs} + \frac{d\boldsymbol{\psi}_{abcs}}{dt}, \ \boldsymbol{\psi}_{abcs} = \mathbf{L}_s \mathbf{i}_{abcs} + \boldsymbol{\psi}_m,$$

$$\mathbf{u}_{abcs} = -\mathbf{r}_s \mathbf{i}_{abcs} + \frac{d\boldsymbol{\psi}_{abcs}}{dt}, \ \boldsymbol{\psi}_{abcs} = -\mathbf{L}_s \mathbf{i}_{abcs} + \boldsymbol{\psi}_m,$$

where $\mathbf{u}_{abcs}$, $\mathbf{i}_{abcs}$ and $\boldsymbol{\psi}_{abcs}$ are the phase voltages, currents and flux linkages; $\mathbf{L}_s$ is the inductance mapping.

The electromagnetic torque is found as

$$T_e = \frac{P}{2}\frac{\partial W_c}{\partial \theta_r} = \frac{P}{2}\frac{\partial}{\partial \theta_r}\mathbf{i}_{abcs}^T \boldsymbol{\psi}_{abcm}.$$

Using the notations reported in [1], the phase windings – magnets coupling is [1]

$$\psi_{asm} = \left[\psi_{m0} + \psi_{m1}\sum_{n=1}^{\infty} a_n \sin^{2n-1}\theta_r + \psi_{m2}\,\mathrm{sgn}(\theta_r)\sum_{k,l=1}^{\infty} a_{l,k}\left|\sin^{\frac{2l-1}{2k-1}}\theta_r\right|\right]$$
$$\circ\left[d_0 + \psi_{m3} e^{\sum_{p=1}^{\infty}\left(a_p \sin^p \frac{1}{c_p}\theta_r + b_p \cos^p \frac{1}{c_p}\theta_r\right)}\right],$$

$$\psi_{bsm} = \left[\psi_{m0} + \psi_{m1}\sum_{n=1}^{\infty} a_n \sin^{2n-1}(\theta_r - \tfrac{2}{3}\pi) + \psi_{m2}\,\mathrm{sgn}(\theta_r - \tfrac{2}{3}\pi)\sum_{k,l=1}^{\infty} a_{l,k}\left|\sin^{\frac{2l-1}{2k-1}}(\theta_r - \tfrac{2}{3}\pi)\right|\right]$$
$$\circ\left[d_0 + \psi_{m3} e^{\sum_{p=1}^{\infty}\left(a_p \sin^p (\frac{1}{c_p}\theta_r - \frac{2}{3}\pi) + b_p \cos^p (\frac{1}{c_p}\theta_r - \frac{2}{3}\pi)\right)}\right],$$

$$\psi_{csm} = \left[\psi_{m0} + \psi_{m1}\sum_{n=1}^{\infty} a_n \sin^{2n-1}(\theta_r + \tfrac{2}{3}\pi) + \psi_{m2}\,\mathrm{sgn}(\theta_r + \tfrac{2}{3}\pi)\sum_{k,l=1}^{\infty} a_{l,k}\left|\sin^{\frac{2l-1}{2k-1}}(\theta_r + \tfrac{2}{3}\pi)\right|\right]$$
$$\circ\left[d_0 + \psi_{m3} e^{\sum_{p=1}^{\infty}\left(a_p \sin^p (\frac{1}{c_p}\theta_r + \frac{2}{3}\pi) + b_p \cos^p (\frac{1}{c_p}\theta_r + \frac{2}{3}\pi)\right)}\right].$$

The electromagnetic systems design is performed with a goal to attain an optimal homogeneous and uniform winding–magnet coupling

$$\boldsymbol{\psi}_m = \begin{bmatrix}\psi_{asm}\\ \psi_{bsm}\\ \psi_{csm}\end{bmatrix} = \psi_m \begin{bmatrix}\sin\theta_r\\ \sin\left(\theta_r - \frac{2}{3}\pi\right)\\ \sin\left(\theta_r + \frac{2}{3}\pi\right)\end{bmatrix}.$$

This is a very challenging problem. A near-optimal nonlinear electromagnetic system design is accomplished. The images of permanent-magnet synchronous machines are shown in Figures 5. These machines are examined, tested and characterized. It is found that up to the peak loadings, the generator induces the sinusoidal or near-sinusoidal phase voltages. Figures 6 illustrate the induced voltages at the balanced and unbalanced loadings for light, rated, peak and maximum *admissible* loads. The experimental results substantiate that the developed technology ensures optimal generator performance, guarantee excellent machine capabilities, as well as uniquely suits the harmonic reduction, power factor correction and energy management schemes.

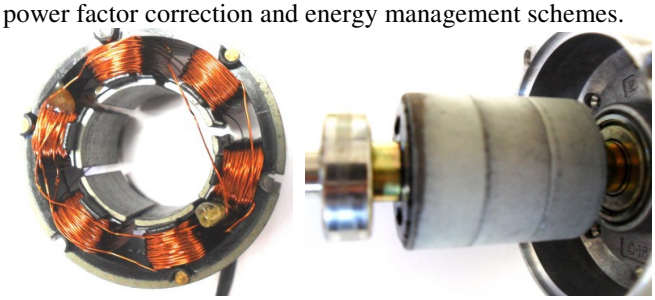

Figure 5. Images of three-phase synchronous machines: Stator with the *as*, *bs* and *cs* phase windings, and, rotor with segmented magnets

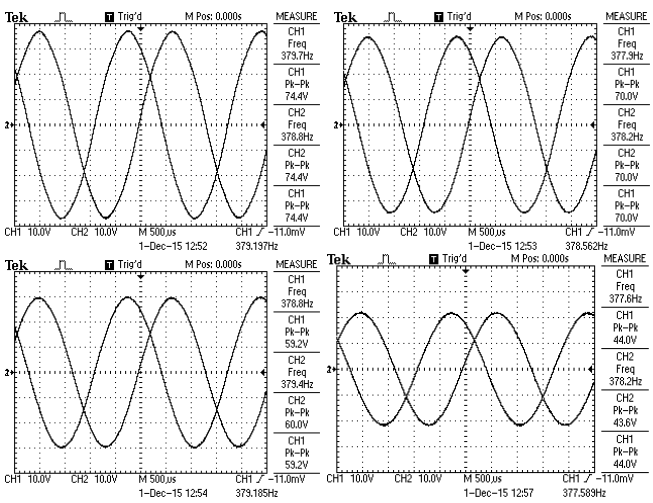

(a)

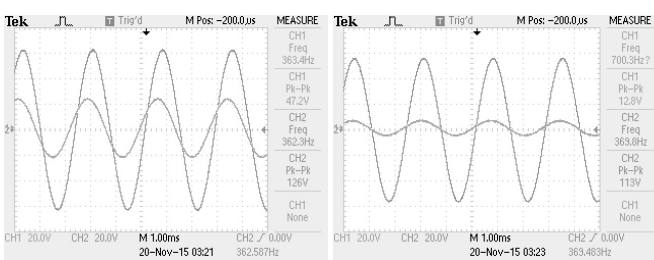

(b)

Figure 6. Induced phase voltages by synchronous generator: (a) Balanced light, rated, peak and maximum *admissible* loads;
(b) Unbalanced rated and peak loads: Near-sinusoidal phase voltages are induced.

5. CONCLUSIONS

This paper focuses on innovative solutions, practical technologies and enabling tools in designing energy-efficient high power density synchronous generators and power generation systems. We applied affordable technologies for current and future electric machines and transducers for energy, power, automotive and aerospace industries. The design solutions and hardware are experimentally verified and substantiated. *Clean* and renewable energy systems are enabled by consistent analysis, design and optimization. Our findings promise one to ensure affordable, *clean* and sustainable technology improvements applied to current and future energy and power systems.

REFERENCES

1. S. E. Lyshevski, *Mechatronics and Control of Electromechanical Systems*, CRC Press, Boca Raton, FL, 2016.
2. S. E. Lyshevski, *Nano and Micro Electromechanical Systems: Fundamentals of Nano and Microengineeirng*, CRC Press, Boca Raton, FL, 2003.
3. L. Masisi, M. Ibrahim and P. Pillay, "Control strategy of a variable flux machine using Alnico permanent magnets," *Proc. Energy Conversion Congress and Exposition*, pp. 5249-5255, 2015.
4. W. Tang, L. Zhou, A. Kassen, A. Palasyuk, E. White, K. W. Dennis, M. J. Kramer, R. W. McCallum and I. E. Anderson, "New Alnico magnets fabricated from pre-alloyed gas atomization powder through diverse consolidation techniques," *Proc. Magnetics Conf.*, pp. 1, 2015.
5. A. S. Rao, "Alnico permanent magnets: An overview," *Proc. Electrical Electronic Insulation and Electrical Manufacturing Conf.*, Chicago, IL, pp. 373-380, 1993.
6. L. Zhou, M. Miller, D. A. Cullen, P. Lu, R. W. McCallum, I. E. Anderson, S. Constantinides and M. J. Krammer, "Microstrutural charaterization of alnico 9 alloy," *Microscopy and Microanalysis*, paper 0671, pp. 1343-1344, 2015.
7. L. Zhou, M. K. Miller, P. Lu, L. Ke, R. Skomski, H. Dillon, Q. Xing, A. Palasyuk, M. R. McCartney , D. J. Smith, S. Constantinides, R. W. McCallum, I. E. Anderson, V. Antropov and M. J. Kramer, "Architecture and magnetism of alnico," *Acta Materialia*, vol. 74, pp. 224-233, 2014.
8. B. Lawn, *Fracture of Brittle Solids*, Cambridge University Press, Cambridge, 1993.
9. E. S. Berkovich, "Three-faceted diamond pyramid for micro-hardness testing," *Ind. Diamond Rev.*, vol,11, no, 127, pp. 129-133, 1951.